Chinese Chemical Letters 33 (2022) 2155–2158

Contents lists available at ScienceDirect

Chinese Chemical Letters

journal homepage: www.elsevier.com/locate/cclet

Hydrophilic carbon nanotube membrane enhanced interfacial evaporation for desalination

Yaqi Hou[a], Qianxiao Wang[a], Shuli Wang[a], Miao Wang[c,*], Xuemei Chen[d], Xu Hou[a,b,e,**]

[a] State Key Laboratory of Physical Chemistry of Solid Surfaces, College of Chemistry and Chemical Engineering, Xiamen University, Xiamen 361005, China
[b] Research Institute for Biomimetics and Soft Matter, Fujian Provincial Key Laboratory for Soft Functional Materials Research, Jiujiang Research Institute, College of Physical Science and Technology, Xiamen University, Xiamen 361005, China
[c] College of Materials, Xiamen University, Xiamen 361005, China
[d] School of Energy and Power Engineering, Nanjing University of Science and Technology, Nanjing 210094, China
[e] Tan Kah Kee Innovation Laboratory, Xiamen 361102, China

ARTICLE INFO

Article history:
Received 20 July 2021
Revised 29 August 2021
Accepted 2 September 2021
Available online 8 September 2021

Keywords:
Hydrophilic surface chemistry
Carbon nanotube
Water evaporation
Desalination
Molecular dynamic simulation

ABSTRACT

Carbon nanotube-based (CNT-based) interfacial evaporation material is one of the most potential materials for solar desalination. Here, we studied the evaporation rate of the CNT-based membranes with different hydrophilic and hydrophobic chemical modified surfaces using molecular dynamic simulations. We found that the hydrogen bonding density among water molecules at the interface is a key factor in enhancing the evaporation rate. For a hydrophilic CNT-based membrane, the strong interactions between the membrane outer surface and the water molecules can destroy the water-water hydrogen bonding interactions at the interface, resulting in the reduction of the hydrogen bonding density, leading to an enhancement effect in evaporation rate. We also found that there is an optimal thickness for evaporation membrane. These findings could provide some theoretical guidance for designing and exploring advanced CNT-based systems with more beneficial performance in water desalination.

Water is the source of life, but only 0.5% of the global water resources are fresh water that can be directly used by humans [1]. The shortage of fresh water has become one of the main threats to the sustainable development of mankind. To meet this challenge, many desalination technologies, such as multi-stage flash evaporation [2] and reverse osmosis [3], have gradually emerged and alleviated water shortages to some extent. However, these traditional desalination technologies generally consume large amount of electricity, oil, or other energy sources, resulting in serious environmental problems. In recent years, the technology of solar-driven interfacial evaporation seawater desalination that obtains fresh water by using green energy has rapidly developed into a sustainable technology with broad prospects [4–7].

As we know, the physicochemical properties of the interfacial materials, especially the surface chemical properties, have a significant impact on the microstructures and phase transition behaviors of the contacting substances at the interface [8–11], so as for solar-driven interfacial evaporations. Thus, finding the proper interfacial evaporation materials and designing the surface chemical properties to improve and optimize the evaporation performance have become a focus in solar-driven desalination technology. A variety of interface materials [12–16], especially for nanomaterials, have shown beneficial effects in efficient solar desalination, because usually nanoconfinements will bring many special transport properties to the fluidic molecules and ions inside [17,18]. For instance, hydrogel network structure can reduce the evaporation enthalpy so that to realize more efficient evaporation [19]. Furthermore, rational design of the porous structure in interface materials can further optimize the pathways for water transport and speed up the evaporation [19,20]. Among these pioneering explorations, carbon nanotube-based (CNT-based) materials have become one of the promising interfacial evaporation materials for solar desalination due to their excellent physical and chemical properties [21–25]. First, CNTs, as a super-black material, have efficient light absorption ability, for example, vertically aligned CNT array could adsorb 99.995% of the incident solar energy [21], and CNTs is a kind of efficient solar-thermal conversion materials [23–25]. Second, CNTs have natural nanoscale channel structures, which provides a large area for evaporation and resistance for ion rejection

* Corresponding author.
** Corresponding author at: State Key Laboratory of Physical Chemistry of Solid Surfaces, College of Chemistry and Chemical Engineering, Xiamen University, Xiamen 361005, China.
E-mail addresses: miaowang@xmu.edu.cn (M. Wang), houx@xmu.edu.cn (X. Hou).

https://doi.org/10.1016/j.cclet.2021.09.007
1001-8417/

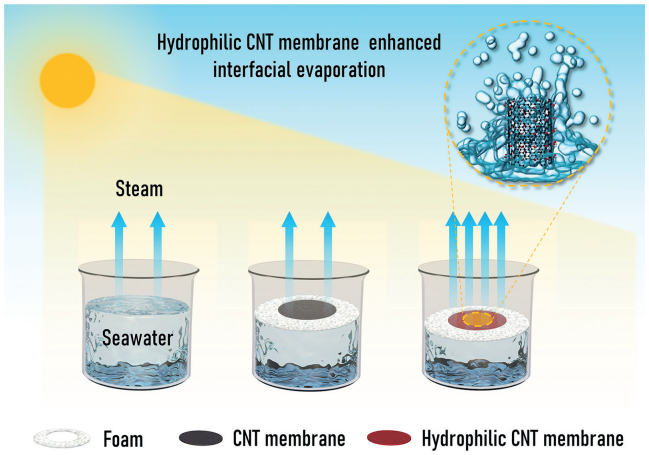

Fig. 1. The schematic diagram of three solar evaporation systems: without evaporation membrane material, with CNT membrane, and with hydrophilic CNT membrane. The hydrophilic CNT membrane can induce more water molecules at the interface to wrap the surface (inset) to produce a larger evaporation surface area so as to facilitate the evaporation process.

[18,22,26,27]. Furthermore, the specific structure of the rim of CNTs can cause the changes in the continuous structure of water-water hydrogen bonding network, which plays a key role in facilitating water transport through CNT membrane [28]. Up to now, the researches on CNT-based materials in seawater desalination mainly focus on the water transport properties inside the channels. The influence of the outer surface on evaporation performance has not been discussed yet. Therefore, exploiting the influence of the hydrophilic and hydrophobic properties of the outer surface of CNTs on the evaporation process is also a key issue worthy of attention.

In this paper, different CNT-based membranes with the hydrophilic and hydrophobic chemical modified surfaces were constructed, and the evaporation rates in different systems were calculated and compared through molecular dynamic simulations using LAMMPS [29]. We found that the hydrogen bonding density among water molecules at the interface is a key factor in enhancing the evaporation rate. The lower the hydrogen bonding density is, the faster the water evaporates. The CNT-based membrane formed by the CNT with hydrophilic outer surface can obviously increase the evaporation area and break the hydrogen bonding interactions (H-bonds) among water molecules due to the strong interactions between the outer surface and water molecules, thus reducing the water-water hydrogen bonding density at the interface, thereby greatly facilitating the evaporation rate. Moreover, the simulation results showed that there is an optimal value for the thickness of the hydrophilic membrane. These findings could potentially spark further experimental and theoretical efforts to design and explore advanced CNT-based systems with superior performance in water desalination.

Fig. 1 shows three solar-driven interfacial evaporation systems. The temperature of the seawater at liquid-gas interface rises due to sunlight, leading to the increase of the thermal motion of water molecules at the interface so that they can break free from the restraints of interactions with other water molecules and vaporize into the air to achieve seawater desalination. As interfacial evaporation membranes, the unmodified CNT membrane is hydrophobic, thus the interaction between the membrane and water molecules is weak, so the influence on the evaporation rate is very limited. However, for the hydrophilic CNT-based membrane after surface modification with hydroxyl (-OH) groups, the interaction with the water molecules becomes strong, the water molecules quickly climb to wrap around the surface of the CNT, which greatly increases the evaporation area of the interface, thereby significantly facilitating the evaporation rate of seawater.

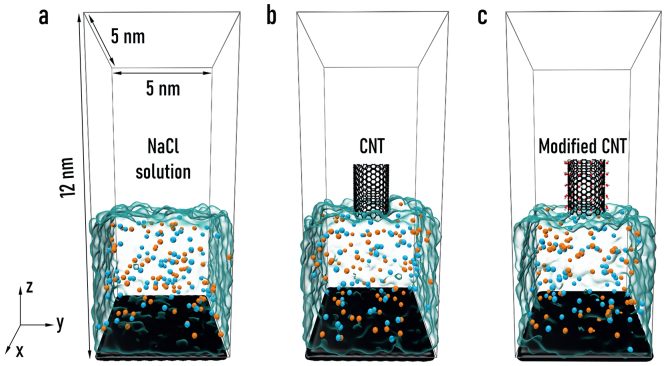

Fig. 2. The illustration of three interfacial evaporation systems used in molecular dynamic simulations. At the liquid-gas interface, there is (a) no interfacial evaporation material, (b) the CNT without surface modification, and (c) the CNT with the hydrophilic surface modified by -OH groups.

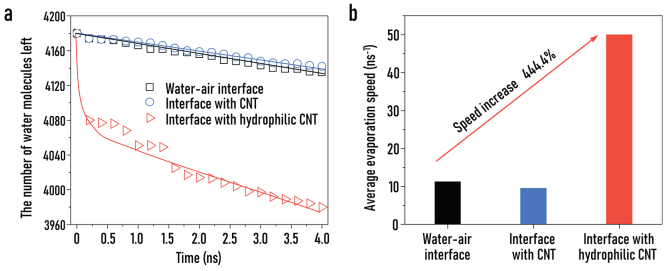

Fig. 3. Comparison of the evaporation rates of the three systems: natural evaporation system without evaporation membrane material, with unmodified CNT as the evaporation material, and with hydrophilic modified CNT as the evaporation material. (a) The amount of water molecules left in the three systems during evaporation processes. (b) The average evaporation rates of the three systems.

In order to further study the detailed microscopic mechanism behind the influence of the hydrophilic and hydrophobic properties of the evaporation material on the seawater evaporation rate, we constructed three simple comparison models as shown in Fig. 2. The bottom part of the model is the bulk phase of 1.0 mol/L NaCl aqueous solution, which is the simplified model for seawater. Sufficient vacuum area is left at the top part of the model for water evaporation and collection. The difference among the three systems lies in the structural design at the liquid-gas interface. In Fig. 2a, there is no evaporation membrane at the interface, which is a natural evaporation system. In Fig. 2b, an unmodified CNT is placed in the center of the interface as the interfacial evaporation material. In Fig. 2c, the interfacial evaporation material is a CNT modified by hydroxyl (-OH) groups. Here, the single CNT model is a partial enlargement of the real interfacial membrane system, which is the smallest structural unit that can represent the characteristic structure of the evaporation membrane. Therefore, the three models are representative for the real interfacial membrane systems. Based on the above three models, the dynamic evaporation processes at high temperature (373.15 K) were simulated and the evaporation rates of the three systems were quantitively calculated. The detailed methods and force field parameters used in the simulations were the same as our previous work [28].

The total number of water molecules left in the systems within a certain period of simulation time is shown in Fig. 3a. After the temperature of system reaches 373.15 K, the number of water molecules left decreases quickly at the initial moment and then decreased linearly over time, with the slope representing the evaporation rate of water molecules. It can be seen that the evaporation rate of water molecules is almost the same in the natural evaporation system and the unmodified CNT system, indicating the hydrophobic evaporation membrane has no significant effect on the evaporation rate of seawater. In contrast, it is obvious that in the

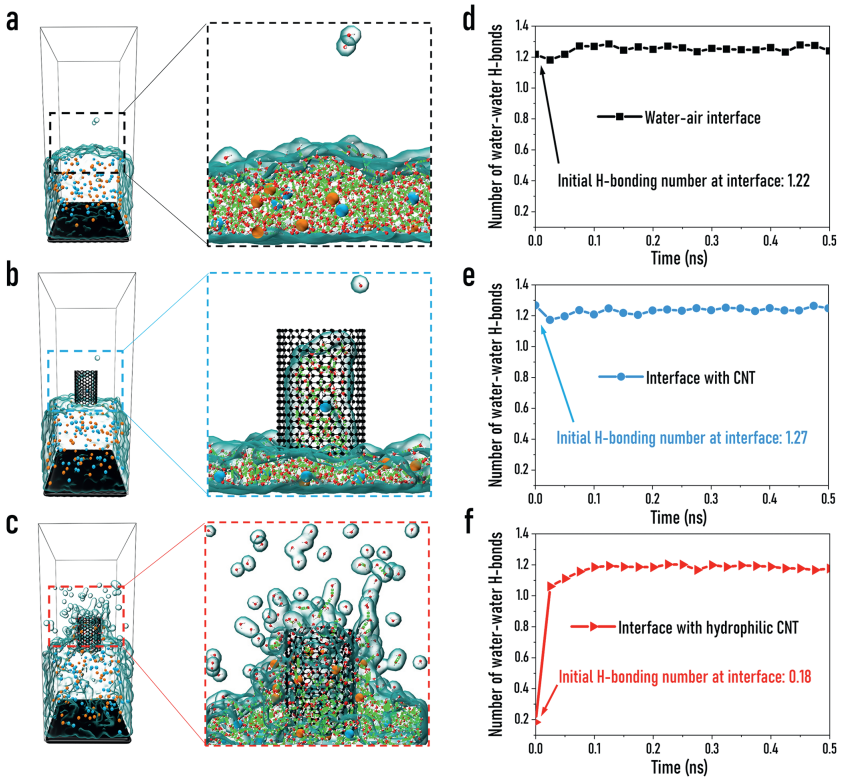

Fig. 4. The microstructure of water molecules at the liquid-gas interface during the evaporation process. The microstructure and hydrogen bonding distribution (shown in green dashed line) of the interfacial water molecules in the (a) natural evaporation system, (b) unmodified CNT system, and (c) hydrophilic modified CNT system. The change in the average number of hydrogen bonding interactions (H-bonds) over time in the (d) natural evaporation system, (e) unmodified CNT system, and (f) hydrophilic modified CNT system. The H-bonds were determined based on the geometrical characteristics [30].

system with the hydrophilic CNT, where the surface is modified by -OH groups, the number of water molecules left decreases significantly compared to the other two systems. From the quantitative results in Fig. 3b, the average evaporation rate of the hydrophilic evaporation membrane system (50 water molecules per nanosecond) is 444.4% larger than that in the natural evaporation system (11.25 water molecules per nanosecond).

To further explore and clarify the microscopic mechanism of the accelerated evaporation rate, we studied the changes in the microstructure of water molecules at the interface during the evaporation of the three systems. Fig. 4 shows the snapshots of the microstructures in the three systems during the evaporation process, we found that the aggregation structures of water molecules at the interface exhibit distinguished differences around the hydrophilic modified CNT compared to that around the hydrophobic CNT.

In the natural evaporation system (Fig. 4a), most of the water molecules still thermally move in the bulk solution phase, and only a few water molecules escape from the water surface and enter the gas phase, so the H-bonds between water molecules at the interface remains dense. When the unmodified CNT is used as the interface material (Fig. 4b), one can see that a small amount of aqueous solution can penetrate the inside of CNT, but the interactions between the CNT and water molecules is weak, thus it has negligible effect on the distribution and microstructure of the liquid phase at the interface. Therefore, it shows the similar phenomenon to the natural evaporation system that only a small amount of water molecules can escape from the interface to the gas phase, and the hydrogen bonding density is as dense as that in the bulk phase. While, when the interface evaporation membrane is the modified CNT, the situation is completely different. It can be seen from Fig. 4c that due to the strong interactions of hydrophilic functional groups with water molecules, a large number of water molecules at the interface wrap onto the outer surface of the CNT, thereby greatly increasing the evaporation area. At the same time, the strong interactions also have a strong influence on the structure of H-bonds among water molecules. Especially for the water molecules wrapping on the membrane surface, of which the H-bonds are destroyed to a large extent, so the water-water hydrogen bond density is significantly reduced.

The water-water hydrogen bond density can be represented by the “number of water-water H-bonds”, that is the number of H-bonds formed by all water molecules at the interface area averaged by the number of water molecules. The changes in the number of water-water H-bonds over the evaporation time have been calculated and shown in Figs. 4d–f. The comparison shows that the unmodified CNT has little effect on the hydrogen bonding density during the evaporation process, while the hydrophilic modified CNT can significantly reduce the average hydrogen bonding density during the evaporation, especially at the initial moment of the simulation, when only ~0.2 hydrogen bonds are formed per water molecule, indicating that the existence of the hydrophilic membrane largely destroys the interactions between water molecules.

Two fragment structures representing the interfacial morphology of CNT surface and water molecules were extracted from dynamic trajectories, based on which the electron density was calculated at B3LYP(D3BJ)/6–311G* level using quantum chemistry software Gaussian 16 [31]. Fig. 5 shows the results of independent gradient model (IGM) analysis [32] based on the calculated electron density using Multiwfn [33]. The visualization was performed by VMD [34]. Almost no water molecules distribute outside the unmodified CNT, and only some water molecules inside form weak van der Waals interactions with the inner surface of CNT. But in the modified CNT system, there are many water molecules distribute outside the CNT and form strong attractions (H-bonds)

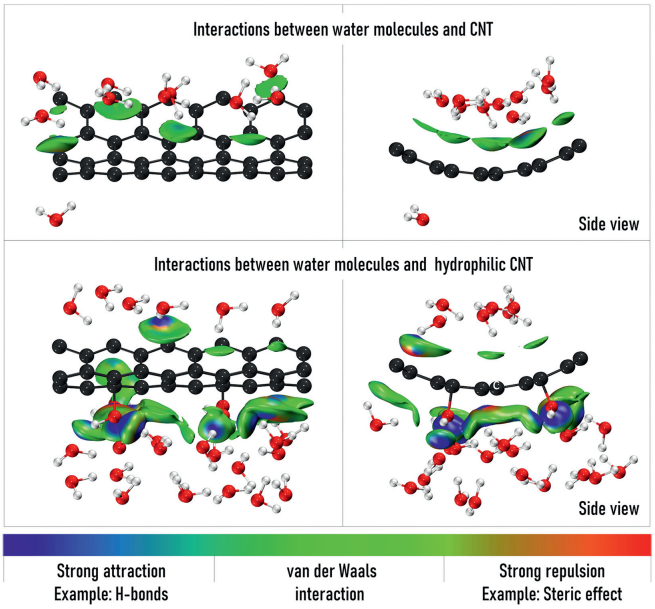

Fig. 5. The IGM analysis of weak interactions between water molecules and CNT surface (isovalue = 0.02).

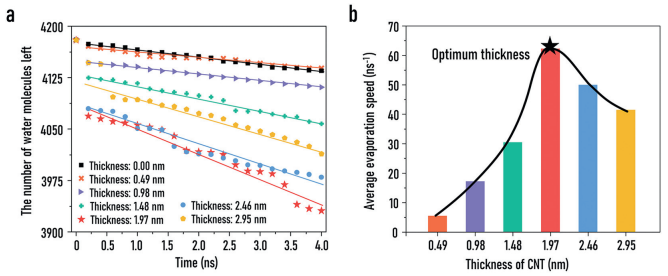

Fig. 6. Comparison of evaporation rates of hydrophilic evaporation membranes with different thicknesses. (a) The amount of water molecules left in the systems during evaporation processes. (b) The average evaporation rates of the hydrophilic evaporation membrane systems with different thicknesses.

with the modified -OH groups, which changes the original orientation of the water molecules, so that the original water-water H-bonds were destroyed and the number of H-bonds between water molecules is greatly reduced. Due to the strong interactions exerted by the modified -OH groups, the reduction of H-bonds greatly reduces the barrier for the liquid-vapor phase transition of water molecules. Therefore, the conclusion can be drawn that the hydrophilic CNT interacts with water molecules, which weakens the H-bonds between water molecules, thus promoting the evaporation of water molecules.

In addition to the hydrophilicity and hydrophobicity of the surface, the thickness of the evaporation membrane is also an indispensable consideration for the design of solar-driven desalination system. Six hydrophilic evaporation membrane systems with thicknesses of 0.49 nm, 0.98 nm, 1.48 nm, 1.97 nm, 2.46 nm and 2.95 nm were built and simulated. As can be seen from the statistical results in Fig. 6, in the evaporation systems of different thicknesses, the reduction rate of the number of water molecules left is significantly different. Furthermore, when the membrane thickness is 1.97 nm, the evaporation rate reaches the maximum value. All these findings indicate that the membrane thickness is indeed an influential factor in evaporation process, and optimizing the thickness of the evaporation membrane is an indispensable consideration for the actual design of an efficient evaporation system.

In this paper, molecular dynamic simulations have been used to compare the evaporation rate of CNT-based evaporation membranes with different surface physicochemical properties, and the microscopic mechanism of the effect of different surface chemical properties on the evaporation rate has been revealed. We found that the hydrogen bonding density among water molecules at the interface is a key factor in determining the evaporation rate. The hydrophilic CNT-based evaporation membrane can yield strong attractions on water molecules so that significantly destroy the water-water H-bonds at the interface, resulting in a great enhancement of the evaporation efficiency. Moreover, the thickness of the evaporation membrane is another influential factor in evaporation process that needs to be optimized in the real desalination system. The results of this paper will further deepen the understanding of interfacial evaporation mechanism and provide new ideas for optimizing the design of CNT-based desalination systems.

Declaration of competing interest

The authors declare that they have no known competing financial interests or personal relationships that could have appeared to influence the work reported in this paper.

Acknowledgments

This work was supported by the National Key R&D Program of China (No. 2018YFA0209500), the National Natural Science Foundation of China (Nos. 52025132, 21975209, 22005255), the Key Laboratory of Biomedical Effects of Nanomaterials and Nanosafety, Chinese Academy of Sciences (No. NSKF202008).

References

[1] T. Humplik, J. Lee, S.C. O'Hern, et al., Nanotechnology 22 (2011) 292001.
[2] J. Zhao, M. Wang, H.M. Lababidi, H. Al-Adwani, K.K. Gleason, Desalination 442 (2018) 75–88.
[3] M. Qasim, M. Badrelzaman, N.N. Darwish, N.A. Darwish, N. Hilal, Desalination 459 (2019) 59–104.
[4] W. He, L. Zhou, M. Wang, et al., Sci. Bull. 66 (2021) 1472–1483.
[5] P. Tao, G. Ni, C. Song, et al., Nat. Energy 3 (2018) 1031–1041.
[6] L. Zhu, M. Gao, C.K.N. Peh, G.W. Ho, Nano Energy 57 (2019) 507–518.
[7] H. Xiong, X. Xie, M. Wang, Y. Hou, X. Hou, Acta Phys. Chim. Sin. 36 (2020) 1912008–1912016.
[8] M. Wang, L. Zhou, Y. Hou, et al., Chin. Chem. Lett. 31 (2020) 1914–1918.
[9] Y. Hou, Y. Ye, Z. Du, et al., Chin. Chem. Lett. 31 (2020) 1640–1643.
[10] Z. Wei, Y. Hou, N. Ning, et al., J. Phys. Chem. B 119 (2015) 9940–9948.
[11] Y. Hou, Y. Ye, Z. Du, C. Zhang, J. Mi, J. Phys. Chem. C 121 (2017) 23763–23768.
[12] L. Zhou, Y. Tan, J. Wang, et al., Nat. Photonics 10 (2016) 393–398.
[13] K.K. Liu, Q. Jiang, S. Tadepalli, et al., ACS Appl. Mater. Interfaces 9 (2017) 7675–7681.
[14] P. Zhang, J. Li, L. Lv, Y. Zhao, L. Qu, ACS Nano 11 (2017) 5087–5093.
[15] J. Zhang, X. Luo, X. Zhang, et al., Chin. Chem. Lett. 32 (2021) 1442–1446.
[16] Z. Li, C. Wang, Chin. Chem. Lett. 31 (2020) 2159–2166.
[17] Y. Hou, X. Hou, Science 373 (2021) 628–629.
[18] M. Wang, Y. Hou, L. Yu, X Hou, Nano Lett. 20 (2020) 6937–6946.
[19] X. Zhou, F. Zhao, Y. Guo, Y. Zhang, G. Yu, Energy Environ. Sci. 11 (2018) 1985–1992.
[20] F. Zhao, X. Zhou, Y. Shi, et al., Nat. Nanotechnol. 13 (2018) 489–495.
[21] T. Yang, H. Lin, K.T. Lin, B. Jia, Sustain. Mater. Technol. 25 (2020) e00182.
[22] M. Wang, H. Meng, D. Wang, et al., Adv. Mater. 31 (2019) 1805130.
[23] Y. Wang, L. Zhang, P. Wang, ACS Sustain. Chem. Eng. 4 (2016) 1223–1230.
[24] E.D. Miao, M.Q. Ye, C.L. Guo, et al., Appl. Therm. Eng. 149 (2019) 1255–1264.
[25] Z. Yin, H. Wang, M. Jian, et al., ACS Appl. Mater. Interfaces 9 (2017) 28596–28603.
[26] H. Yang, Z. Han, S. Yu, et al., Nat. Commun. 4 (2013) 2220.
[27] B. Corry, J. Phys. Chem. B 112 (2008) 1427–1434.
[28] Y. Hou, M. Wang, X. Chen, X. Hou, Nano Res. 14 (2021) 2171–2178.
[29] S. Plimpton, Fast Parallel Algorithms For Short-range Molecular Dynamics, Sandia National Labs., Albuquerque, NM (United States), 1993.
[30] D. Swiatla-Wojcik, Chem. Phys. 342 (2007) 260–266.
[31] M. Frisch, G. Trucks, H. Schlegel, et al., Gaussian 16, Inc., Wallingford CT, 2016.
[32] C. Lefebvre, G. Rubez, H. Khartabil, et al., Phys. Chem. Chem. Phys. 19 (2017) 17928–17936.
[33] T. Lu, F. Chen, J. Comput. Chem. 33 (2012) 580–592.
[34] W. Humphrey, A. Dalke, K. Schulten, J. Mol. Graph. 14 (1996) 33–38.